Study of wall re-deposition on DC-grounded ITER-relevant mirrors with RF plasma in a First Mirror Unit

Kunal Soni[1], Roland Steiner[1], Rodrigo Antunes[1], Lucas Moser[1,2], Pavel Shigin[2], Roger Reichle[2], Laurent Marot[1] and Ernst Meyer[1]

[1] Department of Physics, University of Basel, Klingelbergstrasse 82, CH-4056, Basel, Switzerland
[2] ITER Organization, Route de Vinon-sur-Verdon - CS 90 046 - 13067 St Paul Lez Durance Cedex – France

E-mail: kunaldhirajal.soni@unibas.ch

July 2021

Abstract. In ITER, several first mirrors (FMs) are expected to be DC-grounded with the water cooling lines being implemented as a quarter wavelength ($\lambda/4$) RF-filter. DC-grounding of the FMs can significantly increase the plasma potential V_p, which could trigger an increased wall sputtering and associated re-deposition on the FMs during plasma cleaning. To understand the scope of this impact, helium discharges were excited with DC-grounded FMs in an ITER-sized mock-up of a first mirror unit (FMU) using wall materials with different sputtering energy thresholds (E_th). Additionally, a part of the FM was electrically isolated from the RF to study its impact on the erosion/re-deposition properties on the surface. The E_th of the wall materials, as well as its native oxide layers, had a significant influence on the re-deposition observed on the FMs. With high E_th where walls were unsputtered, both the DC-grounded and electrically isolated parts of the FM were free of deposits. However, with low E_th where the walls were sputtered, there was a net wall re-deposition on the DC-grounded parts of the FM, while electrically isolated parts were still relatively clean. Further, to study the impact of floating wall components, Cu walls in the FMU were isolated from the ground. Here the walls developed a floating potential V_f and the ion energy at the walls was lowered to $\mathrm{e}(V_\mathrm{p} - V_\mathrm{f})$. The floating walls, in this case, were relatively unsputtered and the FMs experienced a net cleaning with total reflectivity of the mirror preserved at pristine mirror levels. This work shows that electrically isolating the FM as well as the wall surface minimizes wall re-deposition in presence of $\lambda/4$ filter and therefore are promising techniques for effective FM cleaning in ITER.

Keywords: RF plasma, DC grounded electrode, notch filter, ITER

Submitted to: *Nucl. Fusion*

1 Introduction

Most optical diagnostic systems in ITER will be equipped with metallic first mirrors (FMs) with the objective of directing the light from the fusion plasma towards the diagnostics through an optical labyrinth in order to prevent neutron leakage. Being the initial elements in the optical diagnostics however, the FMs will be subject to considerable erosion and/or deposition of the first wall materials (beryllium and tungsten) which would significantly degrade their optical properties. The FMs would thus require a periodic cleaning to maintain their optical efficiency, which is foreseen to be achieved by the means of an *in-situ* plasma cleaning technique based on RF discharges [1]. The basis of this cleaning technique is to employ the FM as the powered electrode and feed RF to it directly. The asymmetry in areas of the powered electrode (FM) and counter electrode (grounded wall), leads to a capacitively coupled discharge with the FM acquiring a negative self-bias [2]. This results in the ion bombardment of the FM with a much higher energy (owing to the negative self-bias) in comparison to that on the wall, leading to an effective erosion-dominated cleaning of the FMs. The plasma cleaning of FMs with capacitively coupled discharges has been a subject of numerous studies [3–8].

In addition to the parasitic deposition, the FMs would also be exposed to high thermal loads owing to energetic neutrons and gamma radiation, for which they would require to be actively water-cooled. The physical contact of the metallic and grounded water cooling lines with the FMs leads to grounding of the applied RF. Additionally, ceramics cannot be installed between the FMs and the water cooling pipes in ITER to decouple the ground from the RF. As a coping strategy, the water cooling lines are expected to be implemented in the form of a quarter-lambda filter, commonly known as "notch filter" [10]. This would DC-ground the FMs while allowing the RF to propagate through them, in spite of their physical contact with the grounded water cooling lines [11, 12].

DC-grounding the powered electrode has a significant impact on the properties of the RF plasma and leads to a increase of the plasma potential to several hundred volts (in contrast to a few tens of volts observed in typical highly asymmetric capacitively coupled discharge (CCP)) [13–16]. An explanation of the phenomena was presented by Köhler et al. using a model assuming capacitive sheaths on the powered and the grounded electrode [14,15]. They showed that for DC grounded electrodes, where the self-bias on the electrode $V_{\mathrm{DC}} = 0$, the development of the time averaged plasma potential V_{p} depends exclusively on the sheath capacitances. It also shows that if the area of the grounded electrode is much larger than that of the powered electrode, V_{p} increases to the order of the RF voltage.

The high plasma potential associated with DC-grounding of FMs with a notch filter poses a significant challenge towards plasma cleaning of the mirrors. While the high ion energy (stemming from the high V_{p}) enhances the surface sputtering of the FMs, it also leads to an considerable sputtering of the surrounding walls. The extent of the wall sputtering depends largely on the properties of the incoming ions as well as on the sputtering threshold energy (E_{th}) and yield (Y) of the wall material [17]. Under ITER relevant conditions, a high sputtering of the walls during the plasma discharge is plausible, which would lead to its considerable re-deposition on the FMs. The rate of re-deposition of the wall material (emerging from the sputtering rate of the walls) then competes with the rate of erosion of the FMs, impeding the mirror cleaning process.

The properties of RF plasma with DC-grounded electrodes obtained using a notch filter were investigated in detail in our previous study [18]. In addition to studying the discharges with a conducting electrode, we had also examined discharges with "hybrid electrodes" (with a mixed composition of conducting and insulating surfaces). While the discharge with the conducting electrode led to a high V_{p} of 150 V, running it with the hybrid electrodes led to a lowering of the V_{p} ($115 - 145$ V depending on the ratio of the conducting and the insulating surfaces) and a development of a negative bias voltage V_{DC} on the insulating region of the electrode. The presence of V_{DC} on a specific portion of the electrode led to the ions arriving at the electrode with two particular energies : $\mathrm{e}V_{\mathrm{p}}$ on the conducting surface and $\mathrm{e}(V_{\mathrm{p}} - V_{\mathrm{DC}})$ on the insulating surface.Hence the resulting ion energy is larger on the insulating surface in comparison to the conducting surface. The selective sputtering of the electrode surface with hybrid electrodes is a promising result in perspective of plasma cleaning of FMs in presence of a notch filter, since this points towards an ion bombardment of the FM with a higher energy in comparison to that on the walls when the FM surface is isolated from the electrical ground.

There have been a few reports in literature focused around plasma cleaning of FMs in presence of a notch filter and sputtering of surrounding walls. Dmitriev et al. published results demonstrating the feasibility of notch filter for ITER FM cleaning system using a plasma excited with 81.36 MHz RF and 1 Pa neon gas [19]. They reported a 4 $\mathrm{W\,cm^{-2}}$ RF power density required to achieve an appropriate ion energy in the notch filter scheme which was four times higher in comparison to the DC-decoupled scheme. They also found the notch filter scheme applicable to achieve

removal of Al/Al_2O_3 deposits (used as a proxy for Be/BeO deposits [20]) without degrading the mirror surface using low energy ($\sim 100\,eV$) Ne^+ ions. Chen et al. reported a cleaning of FMs with discharges using a notch filter in the EAST tokamak [21]. Removal of Al_2O_3 deposits from a Mo mirror with Ar plasma in a notch filter configuration was also reported by Moser et al. [4]. Ushakov et al. investigated the re-deposition of surrounding walls during plasma cleaning of FMs without notch filter in the UWAVS test setup using helium plasma [22]. Even at a low ion energy of 20-30 eV, they observed a sputtering and re-deposition of the stainless steel walls on the second mirror in the mock up. In a recent publication, Varshavchik et al. modelled the transport of the sputtered Be particles in weakly ionised helium gas in mirror cleaning experimental conditions relevant to ITER [23]. The simulations showed that transport and re-deposition of the sputtered atoms significantly affect the cleaning efficiency and homogeneity at a few Pa of gas pressure. Further, the simulations pointed towards more pronounced re-deposition with heavier background gas such as neon or argon.

Besides the above mentioned articles, there is a lack of research into the parasitic re-deposition of the walls surrounding the FMs in the presence of notch filter. In this article, we study the impact of the physical properties (E_{th} and Y) as well as the electrical properties (grounded vs floating) of the wall materials on their sputtering and re-deposition on FMs. We also investigate the impact of electrically isolating the powered electrode from the electrical ground on the net wall re-deposition obtained on the electrode surface. All the RF discharges are conducted in presence of a notch filter on the mock-up of a First-Mirror Unit (FMU) relevant to ITER.

2 Experimental

2.1 First mirror unit - Mock up

The experiments were performed in a FMU mock-up placed inside a high vacuum (HV) chamber at the University of Basel (figure 1 of reference [9]). The schematic of the mock FMU is presented in figure 1 and the CAD image of the FMU can be observed in figure 2. The FMU has a square cuboid geometry (250 mm × 150 mm × 200 mm) and holds two unpolished molybdenum (Mo) electrodes (100 mm × 100 mm × 9 mm), M1 and M2, (acting as mirrors) placed in grounded holders on the opposite walls. M1 was used as the powered electrode while M2 was kept either electrically grounded or floating. The body of the FMU was made of aluminium and served as the grounded electrode. A 60 MHz RF generator (Comet cito) coupled with a matchbox was used to generate a 1 Pa helium plasma inside the FMU.

Both M1 and M2 hold three circular insets ($\oslash$ = 26 mm), which could be detached from the mirror for characterization. Two kind of insets were used: (i) bulk stainless steel (SS) insets coated with a thin layer of Mo via magnetron deposition and (ii) bulk Mo insets. The insets could be either electrically connected to the mirror, or electrically isolated from the mirror by placing a 0.3 mm thick insulating ring made of PEEK (Polyether ether ketone) between the mirror and the inset.

The bulk stainless steel insets were coated with Mo via a rotating magnetron in a HV chamber using argon (Ar) as the process gas at 1.82 Pa (base pressure 10^{-4} Pa). A DC plasma generator (ENI RPG-50) was used to excite a plasma on the magnetron with a DC potential and current of 322 V and 0.32 A, respectively on the generator. The deposition rate was measured with a quartz micro-balance (QMB) and was found as 3.4 $Å s^{-1}$. Depending on the duration of the discharge (15 − 24 minutes), Mo films with thickness between 250 nm and 450 nm were deposited on the insets. The slow deposition rate, however, led to presence of oxide and voids in the coating, affecting its density and sputtering yield.

The setup was slightly modified based on the type of experiments performed. To investigate the influence of wall materials (section 3.1), aluminium (Al), copper (Cu) and tungsten (W) were used. To obtain Cu or W bodies, the interior walls of the FMU were lined with 0.5 mm thick Cu or W sheets, respectively. The lining was done via a physical connection ensuring the Cu/W walls were effectively grounded. In these sets of experiments, the influence of RF isolation on M1 was also studied. For this purpose one of the insets (I_{13}) was electrically isolated from the mirror placing the PEEK ring in between. The remaining two insets (I_{11} and I_{12}) were electrically connected to M1. On M2, all the insets were electrically connected. M1 was powered with 60 MHz while M2 was kept floating during the entirety of these experiments.

To study the influence of floating walls (section 3.2), ceramic beads were placed between the Cu sheets and the FMU body to avoid an electrical contact. In these sets of experiments, all the insets were electrically connected in both M1 and M2. M1 was powered while M2 was kept floating or grounded based on the experiment performed.

In the default state of the FMU, the area A_p of the powered electrode (M1) is 100 cm^2, while that of the grounded FMU body, A_g, is 2440 cm^2. Accordingly, the ratio of the grounded to the powered surfaces was $A_g/A_p = 24.4$, which makes the discharge highly asymmetric. In absence of any DC-grounding, the asymmetry of the system results in the development

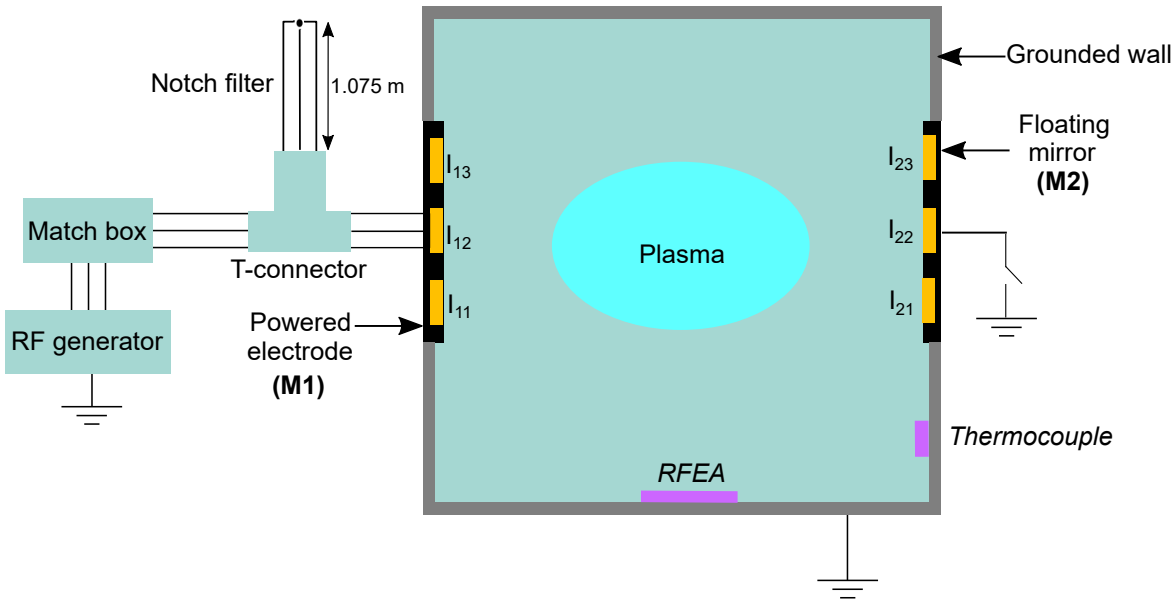

Figure 1. Schematic representation of the experimental setup. The plasma is generated inside the FMU using a 60 MHz generator with a matchbox and the notch filter is connected to M1 via a coaxial T-connector while M2 is floating or grounded depending on the experiment. The characterization devices (Retarding Field Energy Analyser (RFEA), and thermocouple are shown in violet

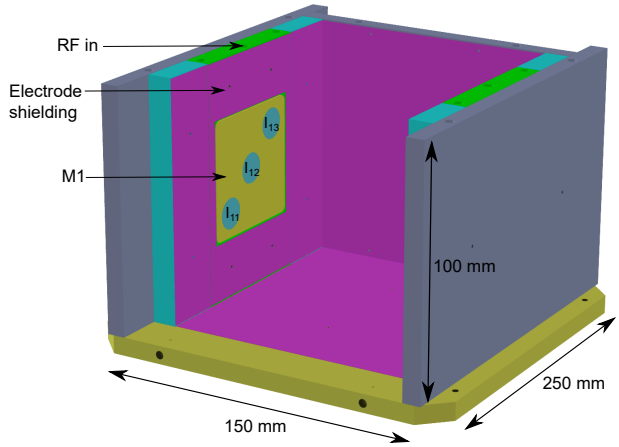

Figure 2. CAD image of the FMU used in the experiments.

of a negative self-bias at M1. However, the DC bias is short circuited by addition of a notch filter at the powered electrode. The length of the notch filter, by definition, is the quarter of the RF wavelength which is 1.25 m at 60 MHz RF. However, the RF propagation speed in the RG 58 cables used for the preparation of the notch filter is roughly $0.86\,c$, with c being the speed of light. Hence the quarter wavelength reduces to $1.25 \times 0.86 = 1.075$ m. Thereby, the notch filter was achieved using a RF transmission line with an electrical

Experimental parameters	*Value*
Area of powered electrode (M1) A_p	100 cm^2
Area of the grounded FMU A_g	2440 cm^2
Notch filter length	1.075 m
Driving frequency	60 MHz
RF power	120 W
He pressure	1 Pa

Table 1. The electrode characteristics and discharge parameters in the experiments.

length of 1.075 m with a short-circuit at one of its ends, while the other end was connected to the system via a T-connector (figure 1). Consequently, a CCP discharge is excited while DC grounding the powered electrode at the same time. The discharge parameters are presented in table 1.

2.2 Characterization techniques

The ion energy distribution function (IEDF) of the ions reaching the wall of the FMU was measured using a Semion^{TM} single sensor Retarding Field Energy Analyser (RFEA) manufactured by Impedans, Ltd [25, 26]. The measurements were analyzed using the Semion System^{TM} software to obtain the IEDF including the ion flux (J_i) and the mean ion energy ($\overline{E_i}$). The typical uncertainties for the measurements in J_i and E_{ion} as provided by Impedans, Ltd are $\pm 20\,\%$ and $\pm 2\,\%$ (in addition to ± 1 eV resolution) respectively. The temperature at the wall over the course of the discharge was measured with a type-K

(Nickel-Chromium / Nickel-Alumel) thermocouple.

The surface chemical composition of the insets was characterized with X-ray photoelectron spectroscopy (XPS). The electron spectrometer is equipped with a hemispherical analyzer (Leybold EA10/100 MCD) and a non-monochromatized Mg Kα X-ray source (hν = 1253.6 eV) was used for core level spectroscopy. The binding energy (BE) scale was calibrated using the Au 4f7/2 line of a cleaned gold sample at 84.0 eV. The fitting procedure of core level line is described in ref [27]. Additionally, the insets were characterised using energy-dispersive X-ray spectroscopy (EDX). Although EDX is widely used as a chemical analysis tool to assess the composition of a sample, this technique also provides information regarding the depth distribution of the chemical species over the first hundreds of nanometers. The depth distribution is studied by performing measurements at different electron energies followed by quantification of the obtained EDX spectrum. The quantification results are then fitted with the STRATAGem software that estimates the amount of specific material of each layer according to the obtained X-ray counts and element properties [28–30]. If the density is known, it can be used to estimate the thickness of the layer. Alternatively, one can use the standard density of the material and obtain an "equivalent" thickness of the layer for the purpose of comparison. The EDX measurements were performed with the SEM-FEI Nova Nano SEM23 microscope, varying the acceleration voltage from 3 to 20 kV. The ex-situ UV-Vis-NIR total and diffuse reflectivity (250–800 nm) of the insets were recorded using a Varian Cary 5 spectrophotometer. The specular reflectivity could be calculated by subtracting the diffuse component from the total reflectivity.

3 Results and discussion

3.1 Influence of grounded wall materials and RF isolation

The experimental results for the discharges in the FMU with different internal walls, Al, Cu and W, are presented in this section. All the wall materials had a considerable resting period in air, leading to a development of a thin oxide layer on the surface. Bulk SS insets coated with Mo were used on M1 and M2.

Prior to conducting the experiments, the plasma was characterized for the discharge parameters mentioned in table 1. The IEDF obtained at the grounded wall displayed a single peak at 90 eV, which corresponds to the high energy limit of the He^+ ions that reach the wall. The surface power density on the electrode M1 was roughly 1 $W\,cm^{-2}$. The measured ion flux at the wall was $9.4\times10^{18}\,m^{-2}s^{-1}$. The RFEA was removed from the FMU after the plasma characterization, to prevent its sputtering and re-deposition on the mirrors during experiments. The experiments involved running a plasma discharge with different wall materials for 7 hours. This corresponds to an ion fluence of $2.4\times10^{23}\,m^{-2}$. Furthermore the temperature of the walls increased progressively from 30°C to 83°C during the experimental run.

Since the powered electrode is DC-grounded, the ions sputter the surfaces of both the electrode as well as the walls with an energy of eV_p = 90 eV in our experiments. In such a scenario, the erosion of the powered electrode competes with a subsequent re-deposition of the wall material during the discharge. The rate of wall re-deposition depends on the multiple factors including the process gas, plasma parameters, sputtering yield of the wall material at eV_p and the geometry of the setup. Hence over the course of the discharge, the electrode can be in an erosion or a re-deposition dominant regime. However, when the surface of the powered electrode is electrically isolated, the flow of DC-current from the plasma to the electrode is blocked at the dielectric, and the surface of the electrode acquires a negative self-bias V_{DC} [18]. As a result, the ions reach and sputter the surface of the electrode with an energy of $e(V_p - V_{DC})$, while they reach the grounded walls with a comparatively lower energy of eV_p. A higher ion energy on the powered electrode can aid shifting the balance to keep the electrode in a net erosion regime. In our experiments, the impact of DC-grounding and electrical isolation of powered electrode was studied via analysing the surfaces of insets I_{11} and I_{13} of M1, respectively. For the sake of clarity, the grounded inset I_{11} and the isolated inset I_{13} in these experiments shall be referred as I_G and I_I, respectively. The V_{DC} on the isolated inset could unfortunately not be measured, since the electrode itself was DC grounded, however from the understanding of results in [18], we estimate it to be in the range of −20 V to −50 V.

Surface characterization was also conducted on the inset I_{22} of M2 to evaluate the extent of wall sputtering. Since M2 was kept floating in the plasma, it acquires the positive floating potential V_f. As a result, the ions reach M2 with an energy of $e(V_p\text{-}V_f)$, which is usually in the range of 10 eV to 30 eV. This energy is considerably low to cause any substantial sputtering on M2. As a result, M2 accumulates all the deposits that reach its surface. Hence, studying the surface of M2 gives a good estimate of the extent of the wall sputtering. The ion energies at the M1, M2 and the wall corresponding to these experiments can be understood in the schematic displayed in figure 3a.

Owing to an exposure in air before XPS measurements, all the surfaces (wall materials as well

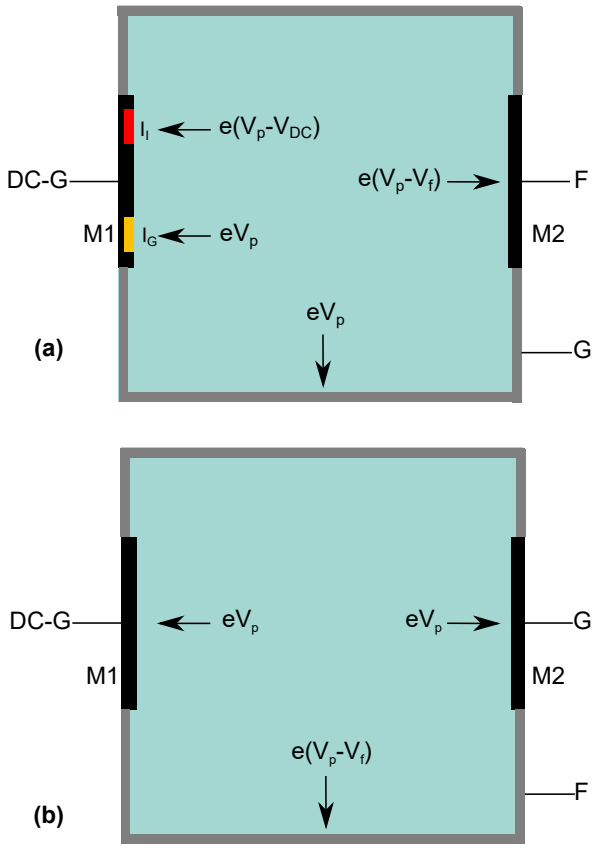

Figure 3. Schematic representation of the ion energies at different components of the FMU in experiments with (a) grounded walls, M1 with grounded (I_g) and isolated (I_I) insets and floating M2, and (b) floating walls, M1 with all grounded insets and grounded M2. DC-G, G and F stand for DC-grounded, grounded and floating, respectively.

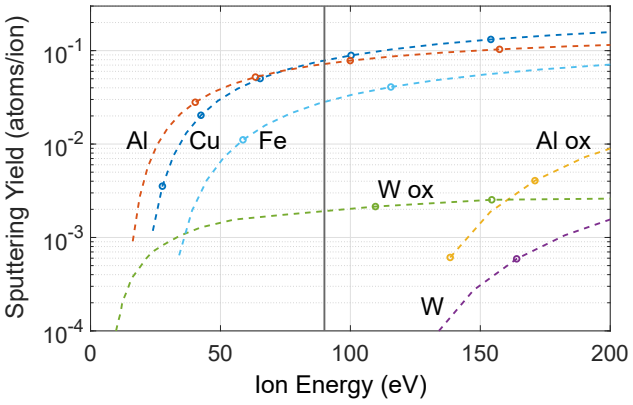

Figure 4. Sputtering yields at room temperature (293 − 303 K) corresponding to a He projectile on different target materials used as the grounded wall in the experiments (obtained from the fitting of the experimental data reported in [31, 32]). Y of iron (Fe) is presented as well, for its relevance to ITER. The vertical line at 90 eV indicates the Y of the wall materials relevant to our experiments. ox in the legend refers to oxide of the corresponding metal.

	Al FMU		Cu FMU		W FMU	
	I_G	I_I	I_G	I_I	I_G	I_I
Mo/oxide	100	100	43.8	94.6	37.8	76.6
Al/oxide	0	0	-	-	-	-
Cu/oxide	-	-	56.2	5.4	-	-
W/oxide	-	-	-	-	62.2	23.3

Table 2. Atomic concentrations (at.%) of the material and their oxide obtained upon the XPS measurements performed on insets I_G and I_I after experiments in the FMU with the different grounded walls.

as insets) had high atomic concentrations of C, N and O (up to 50 at.%). These elements will not be included in the discussions of the XPS measurements. It is also important noting that the presence of oxides on the walls upon sputtering can also lead to formation of oxygen ions. Additionally, the gases constituting the background pressure of 10^{-4} Pa in the HV chamber can lead to ionisation of different species. These additional ion species can also contribute in the sputtering of the walls/FMs and towards the chemical state of the deposits on the FMs.

Al metal has a very low $E_{\rm th}$ of 13.2 eV, and hence considerable wall sputtering and re-deposition on M1 is expected at the ion energy of 90 eV. However, after the experimental discharge, the surface of M1 was visually free of any deposition. The XPS measurements on the insets I_G and I_I detected near zero concentration of Al, hinting towards a low re-deposition on both the grounded and isolated insets. The EDX analysis of the floating electrode M2 displayed a Al deposition of $1-2$ nm in thickness. A small Al deposition points at a lack of wall sputtering which is attributed to native surface oxidation of the Al walls. Al is known to form a thin oxide layer almost immediately upon its exposure to the environment [33] and the oxide has a much higher E_{th} of 113 eV in comparison to 13.2 eV of Al (figure 4).

The erosion on the insets of M1 was obtained by measuring the decrease in the thickness of the surface coating using EDX analysis. The measurements indicated a net erosion on both the insets, I_G and I_I. The erosion measured on the two insets were similar: erosion on I_G was $\sim$ 80 nm while that on I_I was $\sim$ 90 nm. However, due to the nature of the measurements, the uncertainty in erosion can be as high as $\pm$20 nm. Hence we shall focus mainly on the qualitative aspect of the erosion. The net erosion on both insets is understandable owing to the lack of competing re-deposition from the walls.

Following the discharge with Cu FMU, a non-uniform deposition was visible on M1 with majority of the deposition concentrated around the grounded insets I_{11} (I_G) and I_{12}, while the floating electrode M2 was entirely coated with deposits as observed in figure 5c and 5d, respectively. The EDX measurement on

M2 revealed a considerable deposition of Cu on the surface, which upon fitting via STRATAGem yielded a thickness of 35 nm. This points to the fact that Cu wall was actively sputtered during the experiment. As a result, the floating mirror M2 was coated with a layer of Cu with a deposition rate of 5 nm hr^{-1}. This is expected since the peak ion energy on the walls (90 eV) was considerably higher than the E_{th} of copper (21.9 eV). Moreover, Cu exhibits a high sputtering yield of 0.046 atoms/ion with 90 eV He^+ ions (figure 4). Since Cu oxide was present on the walls used in the experiment, this also indicates that the sputtering threshold of Cu oxide lies well below 90 eV. We can also calculate the approximate wall sputtering rate (S.R.) in nm hr^{-1}, using the following relation,

$$S.R. = 3.6 \times 10^6 \times Y_{\text{i}}\, J_{\text{i}} \left(\frac{M}{N_{\text{A}}\, d}\right) \qquad (1)$$

where Y_{i} is the sputtering yield at the mean ion energy, J_{i} the ion flux (m^{-2} s^{-1}), N_{A} the Avogadro's number, M and d, the atomic mass (g mol^{-1}) and density (g cm^{-3}) of the wall material, respectively. From the IEDF measurement and the associated Y_{i} of Cu, we obtain a wall sputtering rate of 18.3 nm hr^{-1}.

Focusing on M1, the XPS measurements on the DC-grounded inset I_G revealed a 56.2 at.% Cu/oxide on the surface, along with 43.8 at.% Mo/oxide, indicating re-deposition dominated regime. The net erosion measured on I_G was $\sim$ 10 nm. This measurement is within the error range, since the erosion is calculated via an EDX analysis with a high error margin. On the other hand, only 5.4 at.% of Cu/oxide was found on isolated inset I_I, compared to 94.6 at.% of Mo/oxide, implying a negligible net re-deposition of the wall material. Moreover, a net erosion of $\sim$ 120 nm is estimated. The results display that electrically isolating the FM surface significantly lowered the wall re-deposition on it and promoted surface erosion.

W metal has a high E_{th} of 155 eV, and hence no sputtering is expected at an ion energy of 90 eV. However, post the experiment with W walls, a considerable amount of W was detected on M2 via EDX as well as XPS. The equivalent thickness of deposited W layer on M2 via STRATAGem was obtained as 10 nm leading to a deposition rate of 1.4 nm hr^{-1}. The measurements clearly implied a re-deposition of W from the walls. This can be attributed to the sputtering of the native W oxide layer on the surface of the W sheets, which is known to have a significantly lower surface binding and sputtering threshold energy than the W metal. There have been a few studies exploring the behavior of W oxide, the presence of which is reportedly known to lower E_{th} of W by a factor of 10 [31, 34–36]. While the energy of He^+ ions in the experiment is sufficient to sputter the thin oxide layer on the surface of the W walls, it would be unable to sputter the W metal beneath the oxide.

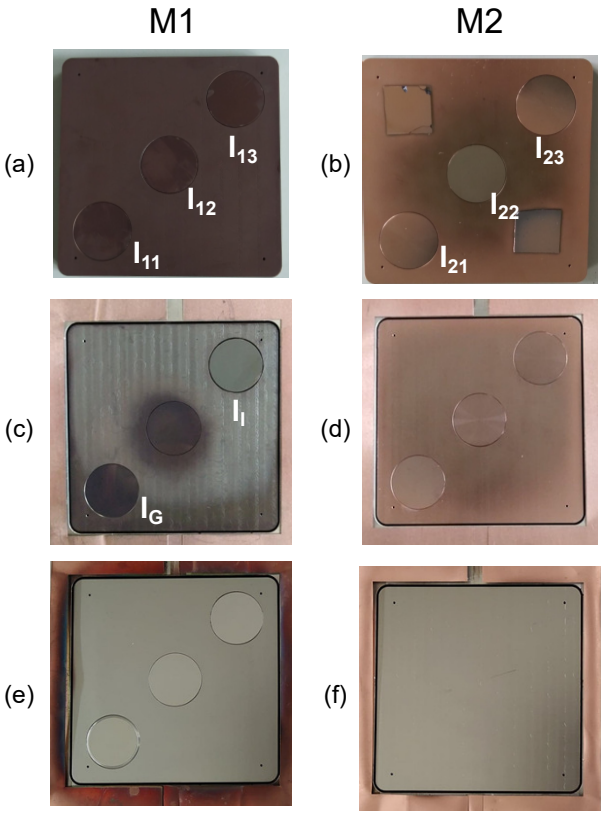

Figure 5. Images of M1 and M2 after experiments in different conditions: (a) M1 with all grounded insets and (b) M2 (floating) in the grounded Cu wall FMU; (c) M1 with two grounded and one isolated inset (I_I) and (d) M2 (floating) in the grounded Cu wall FMU; (e) M1 with all grounded insets and (f) M2 (grounded) in the floating Cu wall FMU.

The XPS measurements on I_G also indicate a re-deposition of W from the walls. It revealed 62.2 at.% of W/oxide on I_G as can be observed in table 2. Furthermore, I_G showcased a reduction in thickness by $\sim$ 10 nm (within the error range). On the isolated inset, I_I, the concentration of W was relatively lower with 23.3 at.% W/oxide, in addition to an erosion of $\sim$ 120 nm. The observation is in line with that obtained for a Cu walled FMU, wherein a lower re-deposition and higher erosion was observed on the electrically isolated inset as well upon wall sputtering. This clearly indicates that the electrical isolation helps shifting the balance of the electrode from a re-deposition dominated regime to an erosion dominated regime, when the walls are sufficiently sputtered. Interestingly, on both I_G as well as I_I, the XPS measurements detect both W and W oxide. One way to explain this could be that the W oxide upon sputtering from the walls is decomposed into W and O, and this W deposits on M1. Furthermore, W on M1 is also unlikely to be sputtered back due to its high E_{th}. It is worth

noting that both the insets were exposed to air before XPS measurements, which could also contribute to oxidation of the re-deposited W.

3.2 Influence of floating wall components

The experimental results for discharges in FMU with floating wall components are presented in this section. Since Cu displayed high etching, it was used as the wall material here to study the re-deposition. Bulk Mo insets were used on M1 and M2 in these set of experiments and all the insets were in electrical contact with the mirrors. Since the erosion on such insets cannot be quantified, we shall focus mainly on the wall re-deposition. The central insets of M1 and M2, I_{12} and I_{22} respectively, were characterised via XPS and EDX after the experiments.

To begin with, the discharge was performed on the FMU with grounded Cu walls and floating M2 to serve as a reference. Since the setup was similar, the plasma properties were also identical to the previous experiments. To recall, the peak ion energy at the walls as well as M1 was 90 eV with a wall sputtering rate of 18.3 nm hr^{-1} from equation 1. M2 was kept floating and the plasma was run for 7 hours. After the experiment, the entire surface of M1 was homogeneously covered with Cu deposits as observed in figure 5a. XPS measurements on I_{12} revealed 66.4 at.% Cu/oxide compared to 33.6 at.% Mo/oxide. Since M2 was floating, it was also coated with Cu deposits as observed in figure 5b.

The atomic concentrations of Cu and Mo on M1 in this experiment is also comparable to that obtained on the inset I_G in Cu FMU (table 2) discussed in the section 3.1. Visual comparison of M1 in the two cases (figure 5a and 5c) further emphasizes the influence of the isolated inset I_I in shifting the erosion/re-deposition balance on M1. Without any isolated insets, M1 is homogeneously in a re-deposition dominated regime (figure 5a), while having one inset isolated influences the erosion/re-deposition balance on the overall electrode (figure 5c). The deposited thickness of Cu on M2 in this experiment (figure 5b) is also similar to that measured on M2 in the Cu FMU in section 3.1 (figure 5d), which is comprehensible owing to similar setup as well as plasma parameters.

To study the impact of floating wall surfaces, the Cu sheets were isolated from the FMU body using ceramic beads. As a result, the inner wall surfaces of the FMU were floating during the plasma discharge. M2, however, was kept grounded in this setup. Moreover, M2 without any insets was used in this experiment to imitate an ITER like FM. The ion energy distribution was studied both at the floating walls as well as grounded M2 in this configuration via a RFEA. The peak ion energy as well as the ion flux measured as a function of the RF power are presented in figure 6. At the floating walls, the peak ion energy remained constant at $\sim$ 30 eV with increasing RF power. This energy corresponds to the $e(V_p - V_f)$ as indicated in figure 3b. It is well known that V_p is related to V_f as follows [37] :

$$V_p - V_f = T_e \log\left(\frac{m_i}{2\pi m_e}\right)^{\frac{1}{2}} \quad (2)$$

where T_e is the electron temperature, m_i the mass of the ion and m_e the mass of the electron. As the RF power is increased, both V_p and V_f increase proportionally, while T_e remains nearly a constant in the range of power used [38]. Hence the difference, $e(V_p - V_f)$ remains roughly a constant as observed in our measurements. Furthermore, since $e(V_p - V_f)$ is roughly 30 eV, this corresponds to $T_e \sim 8.5$ eV as per equation 2, which is in a reasonable limit for T_e of cold He plasma [39].

Since M2 was grounded, the peak ion energy on it increased with increasing RF power. This is well understood since the peak ion energy on M2 corresponds to eV_p and V_p increases with the increasing RF power. As a result, the difference between the peak ion energies at the floating walls and grounded M2 is

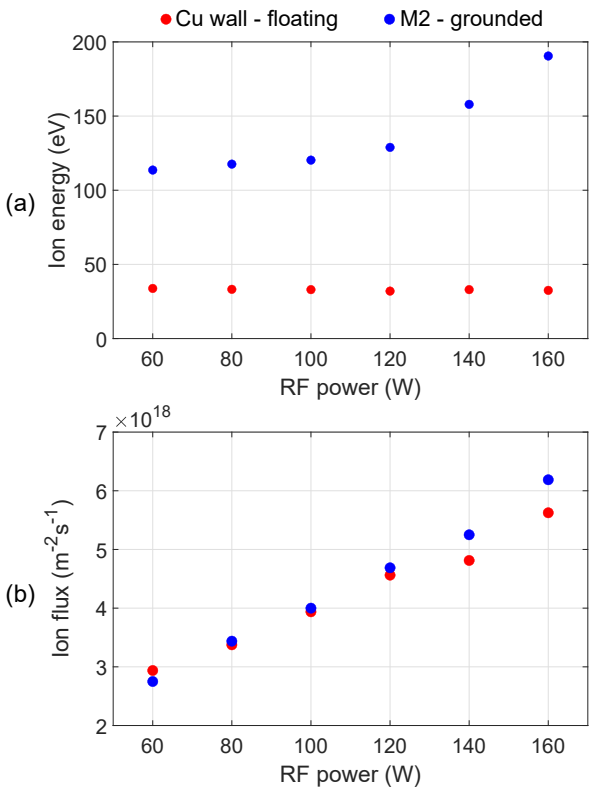

Figure 6. (a) Peak ion energy and (b) ion flux obtained from the experimentally measured ion energy distributions at the floating Cu wall and the grounded M2 as a function of the increasing RF power.

at least 80 eV as can be observed in figure 6a. The ion flux on both the floating walls as well as M2 was comparable and increased linearly with the RF power as observed in figure 6b. A low ion energy at the walls and a high ion energy at M2 with similar ion fluxes, allows for a comparative lower sputtering of the walls than the FMs aiding the plasma cleaning process.

Following the study of the ion energy distributions, a plasma discharge was conducted for 7 hours with the parameters presented in table 1. At 120 W, the peak ion energy at M2 was 128 eV, while that at the floating walls was 32 eV. The ion flux at the two surfaces was around $4.6 \times 10^{18}\,\mathrm{m^{-2}s^{-1}}$. The calculated sputtering rate of the floating Cu walls (from equation 1) was $0.4\,\mathrm{nm\,hr^{-1}}$, which is significantly lower compared to $18.3\,\mathrm{nm\,hr^{-1}}$ with grounded Cu walls used previously. The IEDF was not measured at M1, but is estimated to be similar to M2 since M1 is DC-grounded as well. After the experiment, the surfaces of both M1 and M2 were visually clean as observed in figure 5e,f. XPS measurements on I_{12} displayed a 6.7 at.% Cu/oxide compared to 93.2 at.% Mo/oxide, indicating a negligible wall re-deposition on M1 at the end of discharge. Due to an absence of insets, XPS could not be performed on the surface of M2, however with an EDX measurement, no Cu deposits were detected on M2 suggesting a clean surface.

The reflectivities of the I_{12} from the grounded wall FMU (reference) as well as the floating wall FMU experiment were measured in the wavelength range of 250 nm to 800 nm. Since the reflectivities are more sensitive at lower wavelengths, we shall discuss only the values at $\lambda = 250$ nm. Due to the Cu deposition in the reference experiment (grounded Cu walls), the total reflectivity of the inset was extremely low at 7 % and comparable to the diffuse reflectivity as observed in figure 7. As a result the specular reflectivity was negligible at roughly 1 %. With the floating wall FMU however, the total reflectivity of the inset after the experiment was high at 69 %. A pristine poly-crystalline Mo (PcMo) mirror, unrelated to this experiment, was used as a reference to compare with the reflectivity of the inset. As observed in figure 7, the total reflectivity of the inset was at the pristine PcMo level (72 %). The diffuse reflectivity of the inset was 11 %. This was, however, a result of polishing process of the inset before the experiments and can be minimised with intricate surface polishing. The specular reflectivity of the inset was 58 % compared to 68 % of a pristine PcMo mirror.

The results indicate that using floating wall components can minimise and even eliminate the sputtering of walls, while sufficiently sputtering the FMs during the RF discharges in presence of a notch filter. As a result the FMs can be kept in an erosion dominated regime, allowing for the cleaning of FMs without degrading their reflective properties. The floating wall components hence provide a promising mitigation strategy for RF discharge cleaning of FMs in the presence of a notch filter in ITER diagnostics.

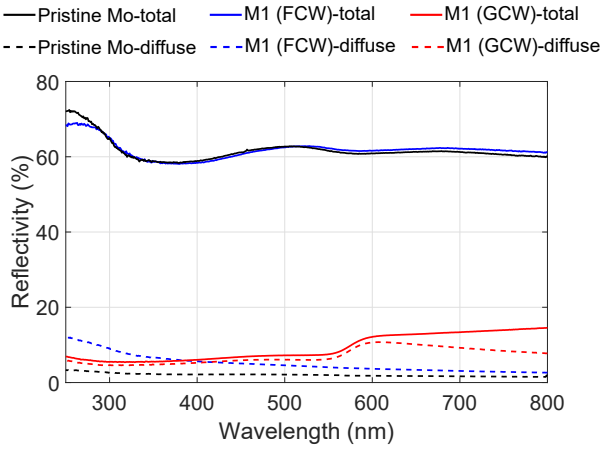

Figure 7. Total and diffuse reflectivities of the inset I_{12} of M1 after experiments in the FMU with the grounded Cu wall (GCW) and the floating Cu wall (FCW). The total and diffuse reflectivities of a pristine poly-crystalline Mo mirror is also presented for reference.

4 Relevance for ITER

The results are of particular importance for the RF plasma cleaning of first mirrors (FMs) in ITER optical diagnostics, where the FMs are foreseen to be DC-grounded with the water cooling lines implemented as a notch filter [10]. DC grounding of FMs will lead to an increase of the plasma potential, and the ensuing wall sputtering will lead to its re-deposition on the FMs, as observed in our results. Consequently, the erosion of the mirror is hindered, making the plasma cleaning process ineffective. While the experiments were done with Al, Cu and W wall materials, the results can also be extrapolated to ITER diagnostic walls, which are expected to be made of stainless steel. The sputtering yield of steel is similar to that of iron [40]. In terms of E_{th} and erosion yield, steel (or iron) is in the range of Cu (figure 4), implying the walls in ITER are prone to significant sputtering and the FMs will be in a predominantly re-deposition regime as observed in our experiments with Cu FMU. This hence necessitates mitigation strategies to counter the wall re-deposition in ITER FMUs.

Electrical isolation of the FM, which leads to a development of a negative self-bias V_{DC} on the FM surface, provides a promising mitigation technique to keep the DC-grounded FMs in a net erosion regime, as observed in our results. Due to the additional bias, the ion energy on the isolated FMs increases to $\mathrm{e}(V_{\mathrm{p}} - V_{\mathrm{DC}})$,

while the walls are sputtered with a lower eV_p. While we only isolated a small portion of the FM, the isolation can be applied on the entire FM in ITER which can further aid in lowering the plasma potential similar to that of a conventional capacitively coupled plasma [18]. This lowering of V_p and the development of a V_{DC} can enhance the mirror sputtering and eliminate the wall re-deposition leading to effective cleaning of FMs even in a DC-grounded configuration.

Isolating the wall components from the ground, which leads to development of a floating potential V_f on the walls also serves as a favourable mitigation technique to minimise and even eliminate the wall re-deposition on the FMs. While the ion energy at the floating walls is nearly a constant at $e(V_p - V_f)$, the ion energy at the grounded FMs eV_p can be sufficiently increased to create optimum conditions for FM erosion in ITER. The wall isolation also allows both M1 and M2 to be cleaned simultaneously in the FMU, while powering only one FM with notch filter. The technique could also be implemented on specific wall portions in ITER FMUs, that have a higher risk of sputtering in different FMU geometries. This would allow to selectively minimise the sputtering of wall portions and subsequently the re-deposition on the FMs.

In ITER, the plasma cleaning is projected to be done in presence of a high magnetic field (3T - 5T depending on the location of the diagnostic system). Presence of magnetic field would have significant implication on the RF plasma and the resulting FM cleaning. However, the mitigation techniques discussed are also relevant for plasma cleaning with notch filter in B field. In the electrical isolation of FM, the presence of B field would have a considerable influence on the V_{DC} developed, due to the confinement of plasma. The plasma is directed in the direction of B field, leading to sputtering of specific portions of the wall. Such portions can be electrically isolated as well, to minimise the wall sputtering. A dedicated study is necessary to investigate the wall sputtering and re-deposition during plasma cleaning with notch filter in B field.

Our results also display that the E_{th} of wall materials can be significantly altered in the presence of surface oxides. This clearly shows that one should consider the state of material following exposure to ambient conditions and account for surface oxides in the wall components of the FMU in ITER. The need to account for the presence of oxide layers on plasma-facing components has been previously identified [41]. Our results also show that W oxide when sputtered from the walls, can get decomposed and deposit as W on the electrode. And in this scenario, the deposited W can remain unsputtered on the mirror if the operating ion energy is less than its E_{th}. This can also have implications for ITER, where W and its oxide (from the divertor) can be deposited on the FMs as well as the FMU walls from the fusion plasma. Here the difference in E_{th} of W and its oxide could significantly influence their re-deposition during the plasma cleaning process. A similar impact can also be deduced for Be and Be oxide deposits (from the first wall) on the FMU walls and FMs, owing to a similar difference in their E_{th} (E_{th} is 16.2 eV for Be, while it is 139 eV for BeO with He projectile).

5 Conclusion and Outlook

In this study we investigate experimentally, the influence of physical and electrical properties of wall materials on their sputtering and re-deposition on DC-grounded electrodes. The experiments were conducted by igniting a helium discharge with a DC-grounded powered electrode (M1) in an ITER sized mock-up of a first mirror unit, where M1 mimicked a first mirror. To study the impact of varying sputtering threshold E_{th} of the walls on the re-deposition obtained on M1, three different metals: copper, aluminium and tungsten, were used as the wall materials. The impact of DC-grounding the electrode on the erosion/re-deposition was studied on one of the insets electrically connected to the electrode, referred to as I_G. Simultaneously, one of the insets was electrically isolated from the powered electrode (referred as I_I) with a thin insulating ring to study its impact on the erosion and re-deposition.

DC-grounding the powered electrode resulted in a discharge with a peak ion energy of 90 eV corresponding to eV_p on the FMU walls. The E_{th} of the walls played an important role in the determination of the erosion/re-deposition balance obtained on the powered electrode. Furthermore, the E_{th} of the Al and W walls was significantly altered by the presence of their native oxides. With the Al body, the walls remained largely unsputtered as a result of native surface oxide which led to a drastic increase of the surface E_{th} from 13.2 eV to 113 eV. On the other hand, with a W body, the walls were sputtered despite a high E_{th} of 155 eV, which was again found to be a consequence of surface oxidation which leads to a significant lowering of its E_{th}.

The re-deposition of the wall materials, when sputtered, significantly impeded the erosion on DC-grounded inset I_G. When the walls were largely unsputtered (in Al FMU), no re-deposition was observed and the inset experienced an erosion of 80 nm. When the walls were significantly sputtered (in Cu FMU), the inset was densely coated with wall re-deposits, while the erosion was negligible. With W FMU, where only the wall oxide layer was sputtered, a W re-deposition was observed on the surface, and the inset experienced no net erosion.

The electrical isolation of RF was observed to reduce the net re-deposition and promote the erosion on the inset I_I. With Al body, the inset eroded by 80 nm without any re-deposition, again owing to lack of wall sputtering. With W body, the re-deposition was significantly reduced in comparison to I_G, and the net erosion increased to 100 nm. A similar effect was observed with Cu walls too, where the Cu re-deposition was drastically reduced on the inset, and the net erosion increased to 120 nm.

To study the influence of floating wall components, the Cu walls were isolated from the ground while the M2 was grounded. The Cu walls in this case developed a floating potential and were sputtered with an ion energy of 30 eV (corresponding to $e(V_p - V_f)$) while the mirrors M1 and M2 were sputtered with a significantly higher ion energy of 128 eV (corresponding to eV_p). However, the ion flux was identical both at the FMs as well as the floating walls. Due to the drastic difference between the ion energies at the mirrors and the walls, both M1 and M2 were considerably eroded while the sputtering and re-deposition from the walls was negligible. The specular reflectivity of the M1 after the experiment was identical to that of a pristine poly-crystalline Mo mirror indicating a preservation of the optical properties post the plasma discharge. In contrast, the experiment with grounded Cu wall led to a homogeneous coating of M1 with Cu deposits and a significant drop in the specular reflectivity to 1 %. A parametric study at varying RF power also indicated that ion energy on the isolated wall ($e(V_p - V_f)$) remained constant while the ion energy at the M1 and M2 increased.

The results call for further work in the plasma cleaning and mitigation techniques when using notch filter. Additional measurements can be performed to be able to conclusively determine whether the mirror is re-deposition dominated or not, such as following the re-deposition thickness evolution with cleaning time. While electrical isolation makes for a promising mitigation strategy, further research is required to understand how the thickness of the isolation as well as the ratio of isolated powered area to DC-grounded powered area impacts the erosion/re-deposition balance on the FMs. The influence of ITER relevant B field on the plasma cleaning and mitigation techniques is also a highly relevant topic for further study, currently under investigation by the authors of this work and whose results will be discussed in a future publication.

6 Acknowledgements

This work was supported by the ITER Organization under I/O Contract IO/18/CT/4300001749. This work has also been carried out within the framework of the EUROfusion Consortium and has received funding from the Euratom research and training programme 2014-2018 and 2019-2020 under grant agreement No 633053. The views and opinions expressed herein do not necessarily reflect those of the ITER Organization or European Commission. Swiss Federal Office of Energy, Swiss Nanoscience Institute, Swiss National Science Foundation and the Federal Office for Education and Science are acknowledged for their financial support.

References

[1] Litnovsky, A., et al. "Diagnostic mirrors for ITER: research in the frame of International Tokamak Physics Activity." Nuclear Fusion 59.6 (2019): 066029.

[2] Chabert, Pascal, and Nicholas Braithwaite. Physics of radio-frequency plasmas. Cambridge University Press, 2011.

[3] Soni, Kunal, et al. "Plasma cleaning of steam ingressed ITER first mirrors." Nuclear Materials and Energy 21 (2019): 100702.

[4] Moser, L., et al. "Towards plasma cleaning of ITER first mirrors." Nuclear Fusion 55.6 (2015): 063020.

[5] Moser, L., et al. "Plasma cleaning of beryllium coated mirrors." Physica Scripta 2016.T167 (2016): 014069.

[6] Dmitriev, A. M., et al. "In situ plasma cleaning of ITER diagnostic mirrors in noble-gas RF discharge." Physica Scripta 2017.T170 (2017): 014072.

[7] Yan, Rong, et al. "Plasma cleaning of ITER edge Thomson scattering mock-up mirror in the EAST tokamak." Nuclear Fusion 58.2 (2017): 026008.

[8] Ushakov, Andrey, et al. "Removing W-contaminants in helium and neon RF plasma to maintain the optical performance of the ITER UWAVS first mirror." Fusion Engineering and Design 136 (2018): 431-437.

[9] Marot, L., et al. "RF discharge mirror cleaning for ITER optical diagnostics using 60 MHz very high frequency." Fusion Engineering and Design 163 (2021): 112140.

[10] Shigin, Pavel, et al. "RF discharge mirror cleaning system development for ITER diagnostics." Fusion Engineering and Design 164 (2021): 112162.

[11] Leipold, Frank, et al. "Cleaning of first mirrors in ITER by means of radio frequency discharges." Review of Scientific Instruments 87.11 (2016): 11D439.

[12] Campbell, David J., et al. "Innovations in Technology and Science R&D for ITER." Journal of Fusion Energy 38.1 (2019): 11-71.

[13] Collins, G. A., and J. Tendys. "Measurements of potentials and sheath formation in plasma immersion ion implantation." Journal of Vacuum Science & Technology B: Microelectronics and Nanometer Structures Processing, Measurement, and Phenomena 12.2 (1994): 875-879.

[14] Köhler, K., et al. "Plasma potentials of 13.56-MHz rf argon glow discharges in a planar system." Journal of applied physics 57.1 (1985): 59-66.

[15] Köhler, K., D. E. Horne, and J. W. Coburn. "Frequency dependence of ion bombardment of grounded surfaces in rf argon glow discharges in a planar system." Journal of Applied Physics 58.9 (1985): 3350-3355.

[16] Aanesland, Ane, et al. "Grounded radio-frequency electrodes in contact with high density plasmas." Physics of plasmas 12.10 (2005): 103505.

[17] Eckstein, Wolfgang. "Sputtering yields." Sputtering by

particle bombardment. Springer, Berlin, Heidelberg, 2007. 33-187.

[18] Soni, Kunal, et al. "Experimental and numerical characterization of a radio-frequency plasma source with a DC-grounded electrode configuration using a quarter-wavelength filter." Plasma Physics and Controlled Fusion 63 (2021): 045005.

[19] Dmitriev, Artem M., et al. "RF plasma cleaning of water-cooled mirror equipped with notch filter based on shorted $\lambda/4$ line." Fusion Engineering and Design (2019).

[20] Marot, Laurent, et al. "Can aluminium or magnesium be a surrogate for beryllium: A critical investigation of their chemistry." Fusion engineering and design 88.9-10 (2013): 1718-1721.

[21] Chen, J. L., R. Yan, and H. Xie. First mirror in-situ cleaning using radio frequency plasma on EAST for ITER edge Thomson scattering system. No. NIFS-PROC–109. 2018.

[22] Ushakov, Andrey, et al. "UWAVS first mirror after long plasma cleaning: Surface properties and material re-deposition issues." Fusion Engineering and Design 146 (2019): 1559-1563.

[23] Varshavchik, L. A., et al. "Three-dimensional simulation of neutral transport in gases and weakly ionized plasmas." Plasma Physics and Controlled Fusion 63.2 (2020): 025005.

[24] de los Arcos, Teresa, et al. "Description of HiPIMS plasma regimes in terms of composition, spoke formation and deposition rate." Plasma Sources Science and Technology 23.5 (2014): 054008.

[25] Schulze, Julian, et al. "The electrical asymmetry effect in multi-frequency capacitively coupled radio frequency discharges." Plasma Sources Science and Technology 20.1 (2011): 015017.

[26] D Gahan et al. "Characterization of an asymmetric parallel plate radio-frequency discharge using a retarding field energy analyzer" 2012 Plasma Sources Science and Technology 21 (2012): 015002

[27] Eren, B., et al. "The effect of low temperature deuterium plasma on molybdenum reflectivity." Nuclear Fusion 51.10 (2011): 103025.

[28] Pouchou, J. L., and F. Pichoir. "Electron probe X-ray microanalysis applied to thin surface films and stratified specimens." Scanning Microscopy International(USA) (1992): 167-190.

[29] Rickerby, David G., and Jean-François Thiot. "X-ray microanalysis of thin film layered specimens containing light elements." Microchimica Acta 114.1 (1994): 421-429.

[30] Galbert, François. "Measurement of carbon layer thickness with EPMA and the thin film analysis software STRATAGem." Microscopy and Microanalysis 13.S03 (2007): 96-97.

[31] Roth, J., Josef Bohdansky, and W. Ottenberger. "Data on low energy light ion sputtering." (1979).

[32] Eckstein, W., et al. "Sputtering Data, Report IPP 9/82." IPP, Garching (1993).

[33] Field, D. J. "Oxidation of Aluminum and its Alloys." Treatise on Materials Science & Technology. Vol. 31. Elsevier, 1989. 523-537.

[34] Guseva, M. I., et al. "Sputtering of beryllium, tungsten, tungsten oxide and mixed W–C layers by deuterium ions in the near-threshold energy range." Journal of nuclear materials 266 (1999): 222-227.

[35] Hijazi, H., et al. "Tungsten oxide thin film exposed to low energy He plasma: Evidence for a thermal enhancement of the erosion yield." Journal of Nuclear Materials 484 (2017): 91-97.

[36] Martin, Céline, et al. "Tungsten oxide thin film bombarded with a low energy He ion beam: evidence for a reduced erosion and W enrichment." Physica Scripta 2017.T170 (2017): 014019.

[37] Lieberman, Michael A., and Alan J. Lichtenberg. Principles of plasma discharges and materials processing. John Wiley & Sons, 2005.

[38] Kechkar, Samir. Experimental investigation of a low pressure capacitively-coupled discharge. Diss. Dublin City University, 2015.

[39] Yaala, M. Ben, et al. "Plasma-activated catalytic formation of ammonia from N2–H2: influence of temperature and noble gas addition." Nuclear Fusion 60.1 (2019): 016026.

[40] Nishi, M., et al. Measurements of sputtering yields for low-energy plasma ions. No. PPPL-1521. Princeton Univ., NJ (USA). Plasma Physics Lab., 1979.

[41] Hodille, E. A., et al. "Retention and release of hydrogen isotopes in tungsten plasma-facing components: the role of grain boundaries and the native oxide layer from a joint experiment-simulation integrated approach." Nuclear Fusion 57.7 (2017): 076019.